

Exploratory Hand: Leveraging Safe Contact to Facilitate Manipulation in Cluttered Spaces

Michael A. Lin^{*1}, Rachel Thomasson^{*1}, Gabriela Uribe¹, Hojung Choi¹ and Mark R. Cutkosky¹

Abstract—We present a new gripper and exploration approach that uses a finger with very low reflected inertia for probing and then grasping objects. The finger employs a transparent transmission, resulting in a light touch when contact occurs. The finger elements are stiff and mounted on precise Cartesian axes for accurate proprioceptive sensing. Experiments show that the finger can safely move faster into contacts than industrial parallel jaw grippers or even most force-controlled grippers with backdrivable transmissions. This property allows rapid proprioceptive probing of objects. Contact information is leveraged to execute grasping actions with a contact-first strategy and to reduce environment state uncertainty. We evaluate a particle filtering algorithm that inputs contact information from either proprioception, or a combination of tactile sensing and proprioception, to estimate object location. Both methods can estimate location within 2 mm; combined tactile sensing and proprioception requires fewer observations.

Index Terms—Perception for Grasping and Manipulation, Grasping, Actuation and Joint Mechanisms, Low-inertia Manipulators, Tactile Exploration.

I. INTRODUCTION

HISTORICALLY, avoiding contact has been synonymous with safety for robotic manipulators. As robots move into unstructured environments such as the home, the definition of safety must be expanded. For a robot to help in spaces such as a kitchen, it must be comfortable with contacts. Constrained, cluttered spaces place kinematic limitations on a robot's ability to find and execute collision-free trajectories. Additionally, home settings are characterized by uncertainty, for instance due to occluded vision, which can lead to unexpected contacts. On the other hand, an advantage of allowing such contacts is that it is a means of sensing the environment through the proprioceptive sensors (i.e. actuator) already present in robots. Contacts can be leveraged to plan motions [1], [2], reduce uncertainty [3], [4], [5], and perform tasks such as object localization [6] and grasp execution [7], [8]. Ensuring that contacts, both planned and unplanned, do not lead to unsafe behavior (e.g. damaging, toppling, or

Manuscript received: October, 15, 2020; Revised January, 24, 2021; Accepted March, 2, 2021.

This paper was recommended for publication by Editor Markus Vincze upon evaluation of the Associate Editor and Reviewers' comments. This work was supported by Toyota Research Institute, National Science Foundation GRFs for R. Thomasson and M. A. Lin, and the Kwanjeong Fellowship for H. Choi.

¹ The authors are with the Department of Mechanical Engineering, Stanford University, Stanford, CA 94305, USA. {mlinyang, rthom, gauribe, hjchoi92, cutkosky}@stanford.edu

* These authors contributed equally to this work.

Digital Object Identifier (DOI): see top of this page.

excessively displacing objects) will enable robot manipulators to more effectively operate in household spaces.

It is difficult to ensure that incidental contacts are safe through controls alone as collisions happen at a short timescale, typically in the 10s of milliseconds [9], often faster than a robot controller's response time, which can be > 100 ms [10]. Limiting maximum speed is a common technique for promoting safety and is often necessary when using commercial robotic grippers, which tend to be heavy and non-backdrivable. This, however, imposes a severe penalty on task speed in cluttered environments.

In this work, we present a robotic gripper equipped with a force-controlled, low inertia finger with Cartesian axes. The finger elements are stiff, but can render low impedances without compromising grasp performance or proprioceptive accuracy. For tasks in which contact occurs at the finger and motion is primarily in the plane of the hand, the effective endpoint mass of the arm/gripper system is dominated by that of the finger, as shown through a macro-mini analysis [11], [12]. The resulting system, even when paired with a conventional industrial robot arm, exhibits a low effective mass compared to either commercial parallel jaw grippers or even typical grippers designed for grasp force control with backdrivable transmissions.

Utilizing this new gripper, the contributions of this work are:

- 1) An analysis of contact forces during collisions as a function of speed and gripper parameters.
- 2) A fast, contact-based grasp primitive that leverages the grippers low inertia and control to quickly acquire objects with position uncertainty.
- 3) An algorithm that uses particle filtering with proprioceptive and tactile sensing to localize objects.

These contributions are combined in a demonstration of an exploration task in which the end-effector leverages contact to localize, infer the properties of, and grasp a target object.

A. Related Work

Grasping Under Uncertainty: The task of grasping under object state uncertainty can be approached through control and mechanical design. Control approaches combine tactile sensing and actuation to create closed-loop behavior that is robust to uncertainty. Pastor et al. developed a method that corrects motion plans based on tactile feedback [8]. Hsiao et al. used state machine flow to find a path, based on contact events, to enclose the object [13]. Murali et al. developed an algorithm to scan for an object based on touch events and

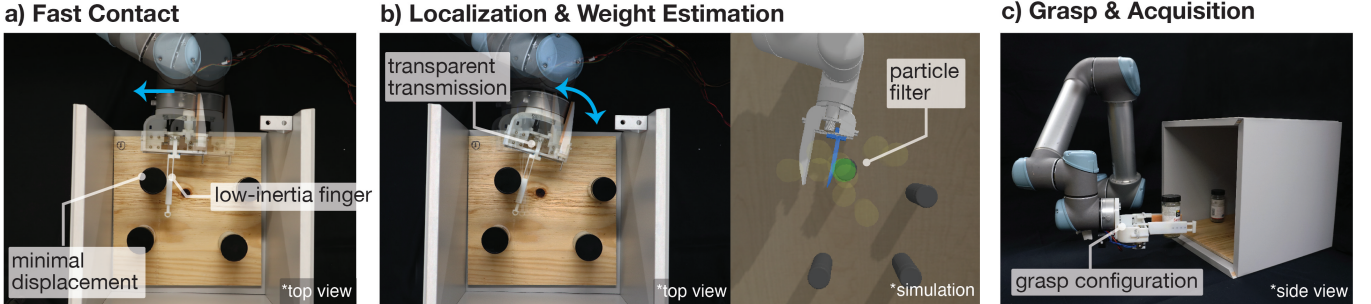


Fig. 1: a) Exploratory Hand reaches into a constrained space to find and grasp the lightest spice jar. b) Low inertia and transparent transmission prevent knocking objects over while gathering information about object location and mass. Particle filtering determines contact locations. c) Stationary “thumb” is moved adjacent to the object and grasp is executed.

generate a grasp candidate based on belief of the object [14]. While these works show promising results, their execution speed is limited because they employ geared industrial grippers which cannot make contact with light or fragile objects both quickly and safely.

Mechanical solutions include exploiting compliance and under-actuation [3], [15], [16], [17]. Piazza et al. provide an extensive review [18]. Grippers in this category enjoy safety benefits as they comply passively, even without backdriving or controlling a motor. However, passive compliance limits proprioceptive accuracy; there is no longer a precise one-to-one mapping from motor to fingertip position.

Exploration Through Touch: Contact information can be useful for estimating the state of unstructured environments. Petrovskaya et al. developed a Bayesian filtering method to determine the pose of known objects to millimeter accuracy based on probed points [6]. A challenge of perception through touch is that it may require many contacts, each of which can be costly in terms of time or risk of displacing the object, thus increasing noise in estimates. Javdani et al. developed an algorithm to select touch actions that maximize information gain [19], but real-time execution can be slow. Others have approached this problem with proximity sensing [7], [20], but such sensors are affected by object surface properties [7]. In nature, many animals use whiskers to safely touch, locate, and explore objects and researchers have adapted such strategies to robots [21], [22]. However, whiskers cannot sense internal object properties and cannot manipulate. In this work, we present an end-effector with an exploratory finger that has low effective mass so as not to disturb objects, similar to a whisker, and is capable of manipulation. This combination reduces the cost of contacts, making tactile exploration practical in cluttered environments.

Low Inertia Manipulators: As noted above, robots that use torque or force/torque sensors to detect collisions cannot respond instantly, leading to high impact forces [10]. For this reason, various papers present low inertia manipulators that are lightweight, structurally stiff, and backdrivable, to minimize forces in the event of a collision [23], [24], [25]. Although fewer examples appear in the literature, a similar paradigm can be applied to robotic hands or grippers, allowing safe collisions similar to soft or under-actuated hands, but without sacrificing proprioceptive precision (e.g. Bhatia et al.’s DDHand [26]).

This motivates their use for exploration in clutter. Our design arises from a similar motivation but offers benefits in terms of its dynamic properties during contact. While the effective mass properties of a linkage-based hand, such as the DDHand, depend both on joint position and location of contact, our design has uniform inertia throughout its workspace and is independent of contact location along the finger. This makes gripper-object interaction more predictable and easy to control during exploration in cluttered environments.

II. TECHNICAL APPROACH

In the following sections we present details of our gripper design. We then show through experiments that the low effective mass and force-transparent transmission can be leveraged for grasping objects based on contact (grasp motion primitive) and 2D localization of objects based on multiple contacts.

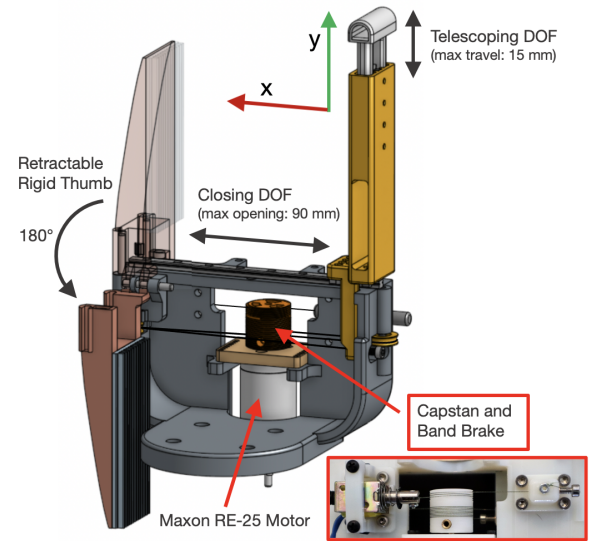


Fig. 2: CAD rendering of gripper with major components and joint limits labeled.

A. Gripper Design

Our goal is a gripper that can quickly and safely contact objects while exploiting accurate proprioceptive sensing to extract information from contact events. To accomplish this,

the Exploratory Hand was designed to have low effective mass in the directions of anticipated contact approach. A consequence, using a macro-mini analysis [11], is that the entire end-point mass of the arm/gripper system is also low, and in fact bounded by the gripper effective mass in the same directions. In addition, a collision involving an articulated body can be reduced to a rigid body collision where the rigid body instantaneously has mass equal to the effective end-point mass of the articulated body [9].

As illustrated in Fig. 2, the gripper uses a single, low-inertia moving finger and a rigid thumb for clamping objects, which can be folded away during phases of exploration. Contacts during exploration of shelves and cabinets will typically occur in the (x, y) plane (as labeled in Fig. 2), and the moving finger achieves low effective mass for contacts in this plane via two perpendicular linear axes. The rail providing motion in the clamping direction is actuated with a low-friction and low-backlash capstan drive. The second rail creates a telescoping prismatic joint using a light spring to passively provide a soft touch for contacts that occur at the tip of the finger while reaching into clutter. As mentioned previously, an advantage of using orthogonal prismatic axes, as opposed to a linkage design, is that the effective end-point mass of the hand is independent of joint position and contact location along the finger.

The following equations are used to calculate the effective mass of a robot arm using our gripper, where $J_v(q)$ is the linear Jacobian, $A(q)$ is the joint-space inertia matrix, $\Lambda_v(q)$ is the task-space inertia matrix, and u is a unit vector along which the effective mass is being measured.

$$\Lambda_v^{-1}(q) = J_v(q)A^{-1}(q)J_v(q)^T \quad (1)$$

$$m_{\text{eff}} = (u^T \Lambda_v^{-1}(q) u)^{-1} \quad (2)$$

An examination of the inertia matrix shows which physical parameters of the gripper contribute to the effective mass:

$$A = \begin{bmatrix} A_{11} & A_{12} \\ A_{12}^T & A_{22} \end{bmatrix}, \text{ where } A_{22} = A_{EH} = \begin{bmatrix} m_x & 0 \\ 0 & m_y \end{bmatrix} \quad (3)$$

$$m_y = m_{\text{tLink}} \quad (4)$$

$$m_x = m_{\text{cLink}} + m_{\text{tLink}} + \frac{I_{\text{rotor}} \cdot N^2 + I_{\text{capstan}}}{r_{\text{capstan}}^2}. \quad (5)$$

where A_{11} and A_{12} contain terms for the robotic arm, A_{EH} is the inertia matrix of the gripper alone, and m_x and m_y are the effective masses of the gripper in the x- and y-directions. The design parameters are the link weights for the telescoping (m_{tLink}) and closing (m_{cLink}) degrees of freedom, the motor inertia (I_{rotor}) and capstan drum inertia (I_{capstan}), the gear reduction (N), and the radius of the capstan (r_{capstan}). Note that N and r_{capstan} are squared, so they dominate the effective mass.

Design details will therefore be informed by the specification of m_{eff} , which depends on the objects that we will contact (how light and how easily toppled over), and on how fast we want the robot to move. An impulse-momentum calculation provides initial insight, but the post-contact behavior also depends on assumptions about the robot and how quickly it

can decelerate. To explore the range of design parameters for the hand we created a collision model in Working Model 2D (Design Simulation Technologies, Inc.) with assumed robot velocities up to 50 cm/s and a light, tippy object (e.g. a cereal box). The maximum permitted m_{eff} to prevent tipping was found for two cases: (i) the finger acted passively after the collision (e.g. under a soft impedance control law) and (ii) a control force rapidly accelerated the finger away from the object after contact. The physical parameters used in the simulation are reported in Table I. The resulting maximum masses were $m_{\text{eff}} = 84$ g and 105 g respectively.

TABLE I: Working Model Analysis Parameters

Coefficients of Static and Dynamic Friction (all bodies)	0.3
Coefficient of Restitution (all bodies)	0.8
Object Width	55 mm
Object Height	260 mm
Object Mass (uniform density)	270 g

3D printed plastic components and structural cutouts allow the finger links to be very light, with $(m_{\text{cLink}} + m_{\text{tLink}})$ at about 40 g. Strict requirements on the mass contribution of the transmission introduce a trade-off between grasp force and effective mass. High gear reductions are common in robotic hands as they allow for high grasp forces without a large continuous current supply to the actuator, which may cause overheating. Our solution uses a low transmission ratio and adds a solenoid-driven band brake to hold peak motor torques. A similar brake design is presented by Siu *et al.* [27]. Using a brushed DC motor with no gear reduction ($N = 1$) and a capstan radius of 10 mm, a peak grasp force of 16 N is achieved. Activating the brake, the sustained force is 11.7 N. This combination of motor and brake allows the gripper to perform delicate grasps (Fig. 3A) but also sustain large forces sufficient for heavier objects (Fig. 3B). For transporting heavy objects, a non-prehensile grasp can also be used in which the robot wrist is rotated so that the weight is borne primarily by the rigid thumb, as shown in Fig. 3C.

The effective mass of the finger in the x-direction is 50.5 g, of which 13.5 g is due to the motor and capstan. The telescoping joint, with a spring providing 42 N/m of restoring force, results in $m_y = 6.56$ g.

As noted earlier, a hand at the end of a robot arm is an example of a macro-mini system [11]. The end-point effective inertia can be visualized as a belted ellipsoid, as shown in Fig. 4. The computation is performed using Eqns. 1 and 2.

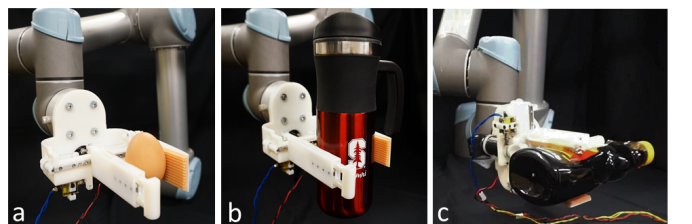


Fig. 3: Exploratory Hand grasping common household objects of different weights and sizes: (a) egg: 56.7 g, (b) coffee mug: 249.2g, (c) maple syrup: 1kg. A non-prehensile grasp is used (c) to carry a heavy object.

The blue (nearly circular for this configuration) ellipse plots the effective inertia of the UR5 robot arm alone, taken at the (x, y) coordinate frame. The orange belted ellipse, shown in detail in the inset, is the combined effective inertia of the macro-mini system for motions in the (x, y) plane. Also plotted, in green, is the effective mass without the telescoping joint, illustrating the value of this passive addition. Table II shows the joint angles used for our calculations. We obtained inertia parameters for the UR5 from the manufacturer provided Universal Robot Description File (URDF).¹ For comparison, human index fingers have an effective end-point mass of $< 0.01 \text{ kg}$ [28].

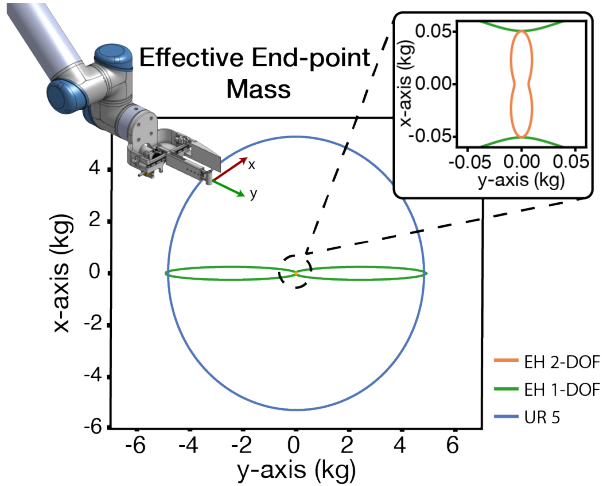


Fig. 4: Effective end-point mass comparison of UR5 alone, Exploratory Hand/UR5 system without telescoping joint (EH 1-DOF) and with telescoping joint (EH 2-DOF).

TABLE II: Joint angles used in effective end-point mass calculation

J1	J2	J3	J4	J5	J6	J7	J8
0°	-55°	91.6°	-38.4°	90°	180°	0	0

Durability: A hand used for tactile probing needs to withstand many collisions. However, cable-driven systems have known limitations, including cable stretch and wear. Additionally, the plastic links are fragile in comparison to metal. In this regard, the very low inertia and backdrivable design are beneficial because collision forces are low even at high speeds, decreasing the likelihood of damage. In the future, glass-filled polymer links can increase durability.

B. System Implementation

The exploratory finger is actuated by a Maxon RE-25 brushed DC motor and controlled with an H-bridge driver and an inline current sensor (Allegro ACS712) for closed-loop current and position control. We use a simple nested control scheme with a PI current controller running at 5 KHz in the inner loop and a PD position controller running at 1 KHz in the outer loop. An embedded microcontroller (Teensy 4.0 Cortex M-7 @600 MHz) is used to execute the controllers and stream

position and current sensor data to a computer at 1 KHz via UART. We use Robot Operating System (ROS) to integrate the gripper with a Universal Robot arm (UR5) to perform all experiments.

III. EXPERIMENTS

A. Impact Forces

In this experiment, we aim to quantify the safety benefits of the Exploratory Hand over designs with higher end-point inertia. We examine the impact forces on objects when making contact at various speeds. In our setup we use a UR5 robot to move a gripper towards the object at constant Cartesian velocity (in the x-direction) while the gripper is not actuated. Forces are measured by coming into contact with a sensorized peg (using an ATI mini-45 Force/Torque (FT) sensor). Measured forces are saturated at approximately 14 N as the peg is designed to separate from the sensor at higher forces to prevent damage.

Five conditions were tested: (a) Exploratory Hand as designed, (b) Exploratory Hand with 200 g additional finger mass, (c) Exploratory Hand using the same motor but adding a gearbox of 26:1 reduction (a typical value for a gripper that is designed to be backdrivable), (d) the Rboroq 2F-85 gripper (a commonly used industrial gripper) and (e) the Rboroq 2F-85 gripper using a commercial FT sensor at the wrist to detect contact. In cases (a-d), we are interested in investigating the significance of effective end-point mass on the exerted force. For these conditions we detect contacts using an interrupt-driven electrical contact sensor where one electrode is on the gripper finger and one is on the peg. This arrangement ensures low latency and high sensitivity to contacts. The case in (e), where contacts are detected when the wrist FT sensor measures a force greater than 0.5 N, is much more common in practice but adds latency due to communication between the wrist, robot, and gripper. The wrist is also subject to noise due to vibrations amplified by the end-effector mass.

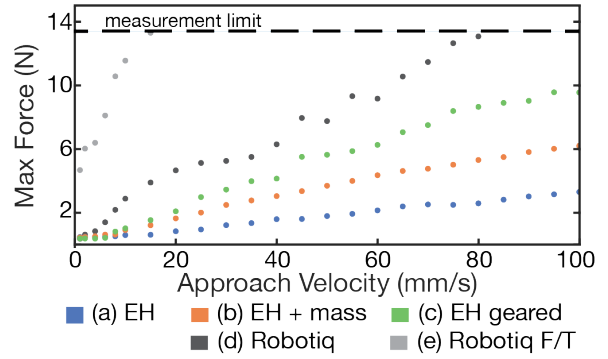


Fig. 5: Plot shows maximum measured forces when making contact at different velocities under each condition: (a) EH as designed, (b) EH with 200 g added mass at finger, (c) EH with a geared motor, (d) Robotiq gripper, (e) Robotiq gripper using only FT sensor to detect contact.

1) Results: Figure 5 plots maximum impact forces as a function of robot velocity. Case (a) shows the lowest impact forces across all approach velocities. For cases (b-d),

¹https://github.com/ros-industrial/universal_robot

we observe increased forces with increasing effective mass. Although the gearbox in case (c) adds little weight, the 26:1 gear ratio results in a large effective mass (≈ 6 kg of motor reflected inertia which, using Eqns. (1-5), results in effective mass of ≈ 4 kg with the UR5) and therefore is worse than adding 200 g mass directly to the finger. For case (e), we observed that forces were large even at low speeds, causing our measurement setup to saturate at speeds >10 mm/s. An examination of impulse, which requires measuring impulse duration with the contact sensor rather than max force, showed a linear relationship between impulse and effective mass, as expected.

2) Discussion: Case (a) results in the lowest impact forces over all speeds due to the very low effective end-point mass of the Exploratory Hand. Cases (b) and (c) show that increasing inertia, either through added mass or an increased gear reduction, leads to higher impact forces, and gearing dominates as the motor inertia reflects through the gearing by N^2 . Grippers often use a high gear reduction to achieve large clamping forces, as is the case with the Robotiq gripper. This results in a high effective mass and the large impact forces seen in cases (d, e). The still larger forces in case (e) are due to the communication latency from the FT sensor (Modbus communication), which was near 30 ms. However, even when contact detection is idealized, as in case (d), impact forces remain large compared to cases (a, b, c). A backdrivable system, such as the Exploratory Hand, reduces the negative impact of communication latencies.

B. Maximum Speed Before Shifting or Toppling Objects

An advantage of maintaining low contact forces is that interactions are less likely to perturb objects, which could increase rather than decrease uncertainty. In cases where pre-existing motion plans depend on the state of the environment, preserving the object location avoids the need to re-plan.

To gain additional insight into gripper-object interactions, we performed experiments in which the robot end-effector collides with free-standing objects at various speeds. In two sets of experiments, we measured the maximum contact speed before the object either slipped > 2 mm in the horizontal direction or toppled over. Object displacement was measured using a mounted camera (Intel® RealSense D435) and AR tags placed on each object (this setup was verified to have error of 0.06 mm on average for small displacements). Parameters for the tested objects are provided in Table III. We conducted two sets of experiments: one with contacts at half the object height, with objects on a wooden surface, and one with contacts near the top of the object, with objects resting on a rubber mat so that they were more likely to tip than slide. Two cases were tested: using the Exploratory Hand as designed (EH), and using the Exploratory Hand with a geared motor (EH geared). Contact was detected using the same electrical contact sensor as in the previous experiment. For each condition we conducted 6 trials. For three trials we started at a low speed and increased the speed by 2 mm/s until the object either slipped or toppled. The other three trials started at a high speed and decremented the speed by 2 mm/s until neither of the failure criteria occurred.

TABLE III: Parameters of objects used for experiments in Sec. III-B

Object	Spice Bottle 1	Spice Bottle 2	Cereal box
Width/Diameter	45 mm	45 mm	55 mm
Height	110 mm	110 mm	260 mm
Weight	40 g	220 g	270 g
Material	Plastic	Plastic	Cardboard

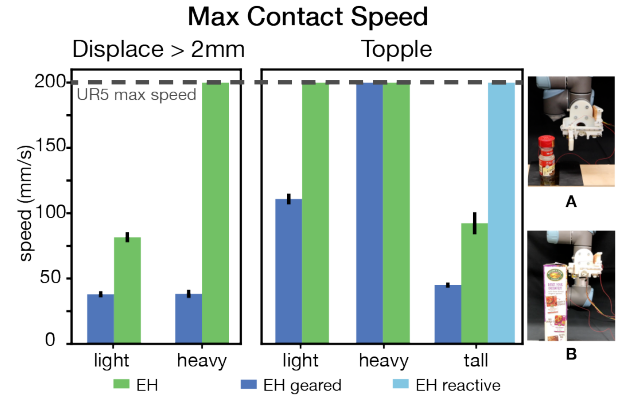


Fig. 6: Left plot shows maximum contact speed before displacing an object by more than 2 mm; right plot shows maximum speed before toppling objects. Tests conducted with UR5 robot and either Exploratory Hand as designed (EH) or EH with a geared motor (EH geared) making contact with light (Spice Bottle 1), heavy (Spice Bottle 2), and tall (Cereal box) objects from Table III free standing on a wood surface (left plot) or a rubber mat (right plot).

1) Results: The results of the experiments are summarized in Fig. 6. In the left bar plot, we observe that for both light and heavy objects, EH can approach with substantially higher speeds (82 mm/s for light and 200 mm/s for heavy) before displacing the object more than 2 mm compared to the EH with motor geared at 26:1 (38 mm/s for both objects). The max speed of the EH case with a heavy object was limited only by the maximum speed of the UR5.

In the right bar plot, we examine cases limited by toppling, with contacts occurring near the top of the object, as shown in Fig. 6AB. In the EH case, speed was limited by the maximum speed of the UR5 robot for all but the tall object for which maximum speed was 92 mm/s. In the EH geared case, maximum speed was 111 mm/s for the light object, 200 mm/s for the heavy object, and 45 mm/s for the tall object.

For the tall object, we also show results from an additional case labeled “EH reactive” (shown as cyan bar). In this case we applied maximum current to the finger motor (bang-bang control) to move it away from the object when contact was detected. With this action we were again able to make contact with the tall object (cereal box) at speeds limited only by the UR5 robot, whereas the non-reactive “EH” case would topple this tall object at an average speed of 92 mm/s.

2) Discussion: For both displacing and toppling criteria, the EH case was able to come into contact at higher speeds compared to the EH geared case. For the EH geared case in the displacement experiment, the maximum speeds for heavy and light objects are similar. We believe this is due to the

significantly higher effective mass which causes an initial impact force large enough to immediately break static friction for objects of either weight. After the object starts to shift, how much it travels is mostly dependent on the speed of the robot and the time it takes for it to stop moving.

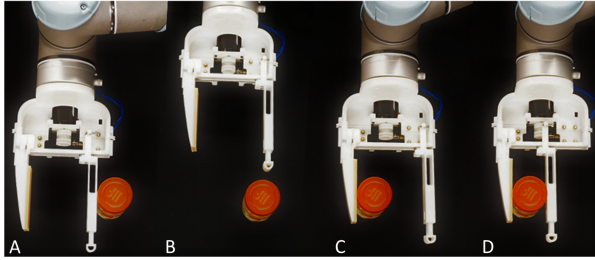


Fig. 7: Contact-based grasp primitive execution begins by approaching an object until making contact with the exploratory finger (A). The contact location is recorded and a motion plan is executed to move around the object (B), placing the rigid thumb at the contact point (C). The exploratory finger closes to complete the grasp (D).

C. Contact-Based Grasp Primitive

The ability to make contact without negative outcomes enables exploration approaches that leverage contact to extract information. For instance, contact information can be used to grasp objects with position uncertainty. We developed a simple grasp primitive that is able to quickly acquire objects based on an initial contact event. The execution (illustrated in Fig. 7) begins by controlling the gripper to hold the finger position with low stiffness and commanding the robot to move at a constant speed toward the expected location of an object such that the back side of the exploratory finger will make initial contact. Contact is detected when the finger is displaced past a distance threshold from its set point position. Upon detecting contact, the location of contact is captured and a sequence of end-effector motions is executed to bring the rigid finger of the gripper in contact with the recorded contact location. Finally, the exploratory finger is commanded to close rapidly and exert a desired grasp force. An advantage of this grasp primitive is that closing the exploratory finger causes little shifting in the location of the object, since the rigid finger is already in contact with the opposite face. This reduces the chance of ejecting or breaking the object during acquisition. Moreover, the entire sequence can be executed at high speeds due to the very low inertia of the exploratory finger.

We verified the performance of the grasp primitive in an experiment where a 141 g spice bottle was manually placed at various locations on a wood surface. The location of the object across trials was determined by a grid pattern where the center of the grid is the expected location, and adjacent placements were spaced every 2 cm. The grasp primitive was executed 5 times per object placement. Not surprisingly, we found that as long as the object location in the direction along the finger was such that the object was within the length of the finger, the grasp would succeed every time. Of the successful trials, the object was shifted an average of 0.83 mm from its

initial pose. Grasps were executed in 1.74 seconds on average after initial contact.

D. Contact-Based Object Localization

Another application of the Exploratory Hand is object localization based on contact information. Due to its low inertia, precise movement, and accurate force control, the finger can touch and stay in contact with objects without displacing them as the end-effector pose changes. As a result, we can move the gripper to different poses causing the contact location to roll along the finger and object (see Fig. 8) while gathering contact measurements. Our approach assumes that the shape of the object is known and, for simplicity, we use cylindrical objects. However, the method is not highly sensitive to errors in assumed object curvature. Objects of other shapes can be incorporated by using contact manifolds [29]. Previous work has shown different methods of using proprioceptive sensing to determine contact point location [30], [5]. These methods perform well under the assumption of a static point contact, however, these point contacts frequently roll and slide as shown in Fig. 8. Conversely, we implemented a particle filtering algorithm that uses a sequence of contact events to measure an object’s state (2D position), taking advantage of the fact that gentle contact measurements do not change this state.

We explore three methods of contact sensing: (i) a “proprioception-only” case where the robot arm and gripper joint positions are used, (ii) a “tactile” case using a custom tactile array in addition to proprioceptive sensing, and (iii) a “hybrid” case which uses tactile sensing only at the moment of contact and only proprioception thereafter. Method (i) has the advantage that it uses a sensing modality available in most robot systems; however, it cannot resolve contact point locations in the direction along the finger. Methods (ii) and (iii) provide coarse information about where contacts happen along the finger (limited by the spatial resolution of the taxels) but require additional integration of sensing hardware. The custom tactile array used in methods (ii) and (iii) is similar to that by Wu et al. [31] with five 10x20 mm taxels arranged in a row with 1 mm separation. A threshold is applied to the sensor signal such that the output indicates binary contact.

The measurement model was different for each contact sensing method. In the proprioception-only method (i) we get very high accuracy measurements of the object location in the direction normal to the finger but no information along the finger. Given this, we define the weight of each particle $w_t^{[m]}$ at time t as follows,

$$s_t^{[m]} = \hat{u} \cdot (x_t^* - x_t^{[m]}) \quad (6)$$

$$w_t^{[m]} = \exp\left(\frac{-s_t^{[m]T} s_t^{[m]}}{2\sigma^2}\right) \quad (7)$$

where \hat{u} is a unit vector normal to the finger, x_t^* is the measured object location at time t (obtained as the center of the contacting finger surface offset by the object radius in the normal direction), $s_t^{[m]}$ is the projected distance of particle m to the measured location, $x_t^{[m]}$ is the state of particle m ,

σ is the standard deviation of the measurement noise. Since proprioception measurement is very precise, σ can be very small (less than 0.1 mm was empirically found to work well). We only perform observation updates when we detect that the finger is in contact.

In the “tactile” method (ii), proprioception information was combined with binary contact sensing at the discrete taxel locations along the finger. A challenge for this method is that the observations have much higher error in the direction along the finger than normal to the finger due to the sensor spatial discretization. To account for this we combined the taxel and proprioception measurements with separate σ values:

$$s_{u,t}^{[m]} = \hat{u} \cdot (x_t^* - x_t^{[m]}) \quad (8)$$

$$s_{v,t}^{[m]} = \hat{v} \cdot (x_t^* - x_t^{[m]}) \quad (9)$$

$$w_t^{[m]} = \exp\left(\frac{-s_{u,t}^{[m]T} s_{u,t}^{[m]}}{2\sigma_u^2} + \frac{-s_{v,t}^{[m]T} s_{v,t}^{[m]}}{2\sigma_v^2}\right) \quad (10)$$

where \hat{u} and \hat{v} are unit vectors normal and along the finger, respectively, x_t^* is the measured object location (center of the active taxel offset in the normal direction by the object radius), $s_{u,t}^{[m]}$ and $s_{v,t}^{[m]}$ are distances of particle m to the measured location projected in the \hat{u} and \hat{v} axes, respectively. σ_u is the standard deviation of measurement in \hat{u} axis and σ_v is the standard deviation in \hat{v} axis (we used $\sigma_u=1$ mm and $\sigma_v=5$ mm). For the hybrid method (iii), we use the tactile array only during initial contact by performing the first 10 updates using method (ii) with $\sigma_u=1$ mm and $\sigma_v=1$ mm. Subsequently, we continue to incorporate contact measurements using the proprioception measurements as in method (i).

To test the localization method, we place a spice bottle at a known location in the robot workspace, execute an end-effector trajectory to make contact, and then rotate about the center of the finger tracking a sine function of 0.2 radians amplitude (shown in the bottom plot of Fig. 8). We used $N=200$ particles, and assumed an arbitrary prior normal distribution of the object location with a mean that was 15 cm away from the ground truth and a standard deviation of 5 cm. Observation

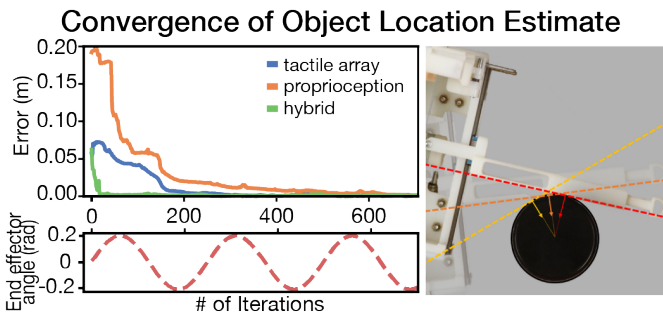


Fig. 8: Left top: Plot shows contact-based object localization convergence using proprioceptive information alone, a binary tactile array, and a hybrid approach with initial updates using tactile array and then switching to proprioception. Left bottom: Plot shows the commanded gripper oscillation. Right: Illustrates rolling motion of the contact during object pose estimation to gather measurements at different orientations.

updates were performed at 100 Hz, but called only when the finger was in contact with the object.

1) Results & Discussion: The results are illustrated in Fig. 8. The proprioception-only, tactile, and hybrid methods converged to final errors of 1.7 mm, 1.3 mm and 0.8 mm respectively. When using proprioception alone, individual measurements provide no information about object location in the direction of the finger. Using a rolling motion, the algorithm combines a sequence of high accuracy measurements at different angles to converge to an estimate within 2 mm in 700 steps. Adding tactile information in method (ii) results in faster convergence. Taking about 300 steps to converge, improvement is limited by the spatial discretization of the tactile sensor, which causes estimates to fluctuate between taxel positions throughout the rolling motion. Converging in 50 steps, the hybrid method (iii) mitigates this issue by using the tactile sensor only initially, to bring the particles near the ground truth, and then refining the estimate using high accuracy proprioception data.

E. System Demonstration

To illustrate how the Exploratory Hand can be used in real-world settings, we performed a system demonstration, illustrated in Fig. 1, in which the hand identifies and acquires the lightest object from a cabinet. First, the exploratory finger sweeps the space until making fast but safe contact with an object, the exact position of which is unknown. The location of the object is then determined using the particle filtering algorithm presented in Section III-D. To determine the relative weight of the objects, the exploratory finger performs a small push of the object and records the force required for displacement. Once this process is repeated for all objects in the scene, the lightest object is grasped using knowledge of its location from the exploratory phase. We assume that the coefficient of friction between each object and the surface is similar.

The main failure case observed was collision of the rigid palm with objects in the environment, introducing uncertainty that could lead to failure of the final grasp. This danger is present when reaching into deep spaces with multiple rows of objects. This demonstration was observed to work reliably when objects were placed in arrangements similar to that shown in Fig. 1, though in general, success depends substantially on how densely packed the objects are.

IV. CONCLUSIONS AND FUTURE WORK

We have investigated the benefits of a precise, low inertia gripper with a transmission that is backdrivable and enables accurate force control for exploration in cluttered environments. We show that reducing the effective mass of the end-effector below a threshold, which depends on the properties of expected objects, enables movement at relatively high speeds in cluttered environments, without danger of substantially perturbing objects. By mitigating the negative consequences of impact, we enable techniques that leverage contact to gain information about the environment. A contact-based grasp primitive is presented for quickly and reliably

acquiring objects with positional uncertainty. Additionally, a particle filtering-based object localization algorithm combines tactile and proprioceptive data to precisely estimate object placement. To show the potential of this new Exploratory Hand for use in real cluttered environments, these techniques are combined for the task of identifying, locating, and acquiring a target object in a cabinet.

As noted in the previous section, an occasional failure case for the cabinet scenario is that the palm of the hand would strike objects first. In the future, controlled pushing motions, as in Dogar et al. [32], could be used to rearrange objects toward the front to enable exploration of objects further back. We plan to incorporate additional sensors in future iterations, including contact sensors on non-grasping surfaces such as the palm and a linear encoder for the passive telescoping joint so that it can be used for proprioception. Moreover, we will explore new designs of the exploratory finger that include multiple actuated joints, enabling more reactivity to sensor readings.

ACKNOWLEDGEMENT

The authors thank Adithya Murali, Arul Suresh, Samuel Frishman and Alexander Gruebele, for very helpful discussions. Toyota Research Institute (“TRI”) provided funds to assist the authors with their research but this article solely reflects the opinions and conclusions of its authors and not TRI or any other Toyota entity.

REFERENCES

- [1] A. Jain, M. D. Killpack, A. Edsinger, and C. C. Kemp, “Reaching in clutter with whole-arm tactile sensing,” *The International Journal of Robotics Research*, vol. 32, no. 4, pp. 458–482, 2013.
- [2] Muhyayuddin, M. Moll, L. Kavraki, and J. Rosell, “Randomized physics-based motion planning for grasping in cluttered and uncertain environments,” *IEEE Robot. and Automat. Letters*, vol. 3, no. 2, pp. 712–719, 2018.
- [3] C. Eppner, R. Deimel, J. Alvarez-Ruiz, M. Maertens, and O. Brock, “Exploitation of environmental constraints in human and robotic grasping,” *The Int. J. of Robotics Research*, vol. 34, no. 7, pp. 1021–1038, 2015.
- [4] L. Manuelli and R. Tedrake, “Localizing external contact using proprioceptive sensors: The contact particle filter,” in *2016 IEEE/RSJ International Conference on Intelligent Robots and Systems (IROS)*, pp. 5062–5069, IEEE, 2016.
- [5] S. Wang, A. Bhatia, M. T. Mason, and A. M. Johnson, “Contact localization using velocity constraints,” in *International Conference on Intelligent Robots and Systems*, 2020.
- [6] A. Petrovskaya and O. Khatib, “Global localization of objects via touch,” *IEEE Transactions on Robotics*, vol. 27, no. 3, pp. 569–585, 2011.
- [7] K. Hsiao, P. Nangeroni, M. Huber, A. Saxena, and A. Y. Ng, “Reactive grasping using optical proximity sensors,” in *2009 IEEE Int. Conf. on Robotics and Automation*, pp. 2098–2105, 2009.
- [8] P. Pastor, L. Righetti, M. Kalakrishnan, and S. Schaal, “Online movement adaptation based on previous sensor experiences,” in *2011 IEEE/RSJ Int. Conf. on Intell. Robots Syst.*, pp. 365–371, 2011.
- [9] S. Ganguly and O. Khatib, “Experimental studies of contact space model for multi-surface collisions in articulated rigid-body systems,” in *Int. Symp. on Experimental Robotics*, pp. 425–436, 2018.
- [10] S. Haddadin, A. Albu-Schaffer, A. De Luca, and G. Hirzinger, “Collision detection and reaction: A contribution to safe physical human-robot interaction,” in *2008 IEEE/RSJ International Conference on Intelligent Robots and Systems*, pp. 3356–3363, 2008.
- [11] O. Khatib, “Inertial properties in robotic manipulation: An object-level framework,” *The Int. J. of Robotics Research*, vol. 14, no. 1, pp. 19–36, 1995.
- [12] S. Ganguly and O. Khatib, “Contact-space resolution model for a physically consistent view of simultaneous collisions in articulated-body systems: theory and experimental results,” *The International Journal of Robotics Research*, vol. 39, no. 10-11, pp. 1239–1258, 2020.
- [13] K. Hsiao, S. Chitta, M. Ciocarlie, and E. G. Jones, “Contact-reactive grasping of objects with partial shape information,” in *2010 IEEE/RSJ Int. Conf. on Intell. Robots and Systems*, pp. 1228–1235, 2010.
- [14] A. Murali, Y. Li, D. Gandhi, and A. Gupta, “Learning to grasp without seeing,” in *International Symposium on Experimental Robotics*, pp. 375–386, 2018.
- [15] Z. Wang, Y. Torigoe, and S. Hirai, “A prestressed soft gripper: design, modeling, fabrication, and tests for food handling,” *IEEE Robotics and Automation Letters*, vol. 2, no. 4, pp. 1909–1916, 2017.
- [16] M. G. Catalano, G. Grioli, E. Farnioli, A. Serio, C. Piazza, and A. Bicchi, “Adaptive synergies for the design and control of the pisa/it softhand,” *The Int. J. of Robotics Research*, vol. 33, no. 5, pp. 768–782, 2014.
- [17] A. M. Dollar and R. D. Howe, “The highly adaptive sdm hand: Design and performance evaluation,” *The International Journal of Robotics Research*, vol. 29, no. 5, pp. 585–597, 2010.
- [18] C. Piazza, G. Grioli, M. G. Catalano, and A. Bicchi, “A century of robotic hands,” *Annual Review of Control, Robotics, and Autonomous Systems*, vol. 2, pp. 1–32, 2019.
- [19] S. Javdani, M. Klingensmith, J. A. Bagnell, N. S. Pollard, and S. S. Srinivasa, “Efficient touch based localization through submodularity,” in *2013 IEEE International Conference on Robotics and Automation*, pp. 1828–1835, 2013.
- [20] T. Schlegl, T. Kröger, A. Gaschler, O. Khatib, and H. Zangl, “Virtual whiskers—highly responsive robot collision avoidance,” in *2013 IEEE/RSJ Int. Conf. on Intell. Robots Syst.*, pp. 5373–5379, 2013.
- [21] J. H. Solomon and M. J. Z. Hartmann, “Artificial whiskers suitable for array implementation: accounting for lateral slip and surface friction,” *IEEE Transactions on Robotics*, vol. 24, no. 5, pp. 1157–1167, 2008.
- [22] M. J. Pearson, A. G. Pipe, C. Melhuish, B. Mitchinson, and T. J. Prescott, “Whiskerbots: A robotic active touch system modeled on the rat whisker sensory system,” *Adaptive Behavior*, vol. 15, no. 3, pp. 223–240, 2007.
- [23] Y.-J. Kim, “Design of low inertia manipulator with high stiffness and strength using tension amplifying mechanisms,” in *2015 IEEE/RSJ Int. Conf. on Intell. Robots Syst.*, pp. 5850–5856, 2015.
- [24] M. Zinn, B. Roth, O. Khatib, and J. K. Salisbury, “A new actuation approach for human friendly robot design,” *The international journal of robotics research*, vol. 23, no. 4-5, pp. 379–398, 2004.
- [25] S. Robla-Gómez, V. M. Becerra, J. R. Llata, E. Gonzalez-Sarabia, C. Torre-Ferrero, and J. Perez-Oria, “Working together: A review on safe human-robot collaboration in industrial environments,” *IEEE Access*, vol. 5, pp. 26754–26773, 2017.
- [26] A. Bhatia, A. M. Johnson, and M. T. Mason, “Direct drive hands: Force-motion transparency in gripper design,” in *Robotics: Science and Systems*, 2019.
- [27] A. F. Siu, M. Sinclair, R. Kovacs, E. Ofek, C. Holz, and E. Cutrell, “Virtual reality without vision: A haptic and auditory white cane to navigate complex virtual worlds,” in *Proc. of the 2020 CHI Conference on Human Factors in Computing Systems*, pp. 1–13, 2020.
- [28] A. Z. Hajian and R. D. Howe, “Identification of the Mechanical Impedance at the Human Finger Tip,” *Journal of Biomechanical Engineering*, vol. 119, pp. 109–114, 02 1997.
- [29] M. C. Koval, M. R. Dogar, N. S. Pollard, and S. S. Srinivasa, “Pose estimation for contact manipulation with manifold particle filters,” in *2013 IEEE/RSJ Int. Conf. on Intell. Robots Syst.*, pp. 4541–4548, 2013.
- [30] M. Kaneko and K. Tanie, “Contact point detection for grasping an unknown object using self-posture changeability,” *IEEE Transactions on Robotics and Automation*, vol. 10, no. 3, pp. 355–367, 1994.
- [31] X. A. Wu, T. M. Huh, A. Sabin, S. A. Suresh, and M. R. Cutkosky, “Tactile sensing and terrain-based gait control for small legged robots,” *IEEE Transactions on Robotics*, vol. 36, no. 1, pp. 15–27, 2019.
- [32] M. R. Dogar and S. S. Srinivasa, “A planning framework for non-prehensile manipulation under clutter and uncertainty,” *Autonomous Robots*, vol. 33, no. 3, pp. 217–236, 2012.